CONTROL CONCEPTS FOR ACTIVE MAGNETIC BEARINGS

R. SIEGWART[1,2], D. VISCHER[1], R. LARSONNEUR[1,2],
R. HERZOG[1], A. TRAXLER[2], H. BLEULER[1], G. SCHWEITZER[1]
[1] Mechatronics Lab, Swiss Federal Institute of Technology (ETH), 8092 Zürich, Switzerland
[2] MECOS Traxler AG, CH-8400 Winterthur, Switzerland

Active Magnetic Bearings (AMB) are becoming increasingly significant for various industrial applications. Examples are turbo-compressors, centrifuges, high-speed milling and grinding spindles, vibration isolation, linear guides, magnetically levitated trains, vacuum and space applications. Thanks to the rapid progress and drastic cost reduction in power- and micro-electronics, the number of AMB applications is growing very fast.

Industrial use of AMBs leads to new requirements for AMB-actuators, sensor systems and rotor dynamics. Especially desirable are new and better control concepts to meet demands such as low cost AMB, high stiffness, high performance, high robustness, high damping up to several kHz, vibration isolation, force-free rotation and unbalance cancellation.

This paper surveys various control concepts for active magnetic bearings and discusses their advantages and disadvantages. Theoretical and experimental results are presented.

1. INTRODUCTION

Basics and feasibility of Active Magnetic Bearings (AMBs) were first shown by Beams, Young and Moore in 1946 [Beams et al. 46]. Considerable progress has been made since, though the basic principle is still the same.

This basic principle gives no general information on how the displacement is measured, how the controller is designed or how the AMB-actuator (electromagnetic coil) is controlled.

Up to now, most AMB-systems made use of ***current*** amplifiers to drive the electromagnetic coils and mainly ***analog PD / PID controllers*** were applied.

For todays and tomorrows demanding AMB-applications, new ***control concepts*** for the actuator and the main controller have to be taken into consideration.

The AMB controller design can be divided into two levels. The first level involves the choice of the input and output variables of the AMB-actuator. This can be denoted as the "***actuator control configuration***". The following rough classification can be made:

- current control
- voltage control
- flux measurement and flux density control
- "self-sensing" control (operation without displacement sensor)

The second level is concerned with the "***main controller***" itself, i.e. the relation between measured signals and actuator input signals. Design approaches for the main controller are:

- PD, PID (root locus)
- LQR, LQG, pole placement (observer based)
- direct low order controller design (SPOC-D, chapter 4.3)
- H^{∞} and other frequency-domain methods

Furthermore, a so called "*feed forward controller*" can be added to the standard feedback loop. This subject is not addressed in this paper.

Prior to the choice of the actuator control configuration and the controller layout, the AMB-engineer should carefully analyze and optimize the configuration of the plant (rotor). The configuration of the plant is basically given through the observability, the controllability, the structural dynamics and the AMB-actuator design [Keith et. al 90], [Siegwart et al. 90]. These aspects are not addressed in this paper.

Starting with the general model of the AMB-actuator (section 2), different actuator control configurations are outlined (section 3). The principles of current, voltage, flux-density and self-sensing control are described, and their advantages and disadvantages are discussed.

Section 4 gives a general overview on the design specifications of the main controller and the different controller layout approaches. PD/PID controllers are widely used low order controllers for applications where performance requirements are not very demanding. For high performance requirements, observer based LQR/LQG regulators are well suited. However, there is still a computational on-line burden because of high order and full coupling in the MIMO case. To close the gap, a tool for direct low order controller design (SPOC-D, chapter 4.3) is shown. Demanding applications, e.g. high performance control of flexible shafts, lead to sophisticated control specifications, mostly in frequency domain. This is the motivation for H^∞ control (chapter 4.4).

Some of the new concepts for actuator control configurations and main AMB controller design discussed in this paper are already used at the Swiss Federal Institute of Technology (ETH) and by the Swiss AMB system manufacturer MECOS Traxler AG. Theoretical and experimental results are presented in section 5.

2. THE BASIC AMB-EQUATIONS

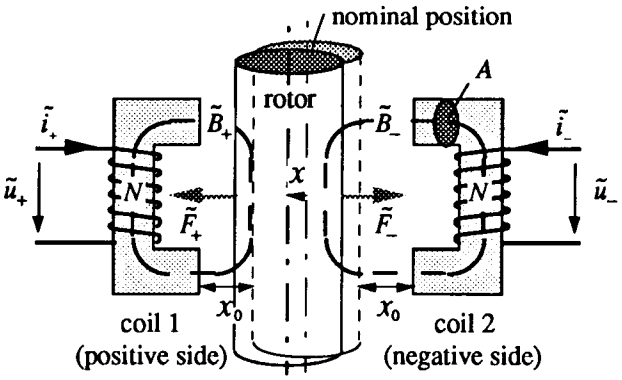

***Figure 1:** Notations for a two-sided actuator with one mechanical degree of freedom, rotor displacement x . A displacement to the left is defined positive, for x=0 the air gaps are x_o. More symbols are listed in table 1 on the next page.*

The basic AMB equations are obtained from Maxwell's laws [Breinl 80], [Traxler 85], [Vischer 88]. The derivations are not shown here. Neglecting secondary effects such as copper resistance, stray fields and saturation, and assuming that the complete energy of the magnetic field is concentrated within the active air gap, we get the following well-known equations for an AMB:

According to figure 1 and to the notation in table 1 we find an electromagnetic force F proportional to the square of the current i in the coil divided by the air gap. The force can also be described by the flux density B.

$$\tilde{F}_+ = \frac{N^2 A \mu_0}{4} \frac{\tilde{i}_+^{\,2}}{(x_0 - x)^2} = \frac{A}{\mu_0} \tilde{B}_+^{\,2}$$

$$\tilde{F}_- = \frac{N^2 A \mu_0}{4} \frac{\tilde{i}_-^{\,2}}{(x_0 + x)^2} = \frac{A}{\mu_0} \tilde{B}_-^{\,2} \qquad (2.1)$$

The relation for the voltage u in the coil can be found as

$$\tilde{u}_+ = \frac{N^2 A \mu_0}{2} \frac{\mathrm{d}}{\mathrm{d}t}\left(\frac{\tilde{i}_+}{x_0 - x}\right) = NA \frac{\mathrm{d}}{\mathrm{d}t}\left(\tilde{B}_+\right)$$

$$\tilde{u}_- = \frac{N^2 A \mu_0}{2} \frac{\mathrm{d}}{\mathrm{d}t}\left(\frac{\tilde{i}_-}{x_0 + x}\right) = NA \frac{\mathrm{d}}{\mathrm{d}t}\left(\tilde{B}_-\right) \tag{2.2}$$

Usually AMB actuators are operated around a constant operating point. The operating point is defined through the following nominal values:

$$x_0,\ i_0,\ B_0 = \frac{N\mu_0}{2}\frac{i_0}{x_0},\ u_0 = 0$$

Around the operating point the relations for the AMB actuator can be linearized for $x \ll x_0$ and $i \ll i_0$:

$$\tilde{F}_+ = \frac{L_0}{2}\frac{i_0^2}{x_0} + \frac{L_0}{2}\frac{i_0^2}{x_0^2}x + \frac{L_0}{2}\frac{i_0}{x_0}i_+ = \frac{A}{\mu_0}B_0^2 + \frac{2A}{\mu_0}B_0 B_+$$

$$\tilde{F}_- = \frac{L_0}{2}\frac{i_0^2}{x_0} - \frac{L_0}{2}\frac{i_0^2}{x_0^2}x + \frac{L_0}{2}\frac{i_0}{x_0}i_- = \frac{A}{\mu_0}B_0^2 + \frac{2A}{\mu_0}B_0 B_- \tag{2.3}$$

$$u_+ = \frac{\mathrm{d}}{\mathrm{d}t}\left(L_0\frac{i_0}{x_0}x + L_0 i_+\right) = NA\frac{\mathrm{d}}{\mathrm{d}t}B_+$$

$$u_- = \frac{\mathrm{d}}{\mathrm{d}t}\left(-\frac{i_0}{x_0}L_0 x + L_0 i_-\right) = NA\frac{\mathrm{d}}{\mathrm{d}t}B_- \tag{2.4}$$

By arranging the AMB in axially opposed pairs of coils (figure 1), as it is usually done, the linearized force F and voltage u result in

$$F = \tilde{F}_+ - \tilde{F}_- \quad = 2L_0\frac{i_0^2}{x_0^2}x + 2L_0\frac{i_0}{x_0}\left(\frac{i_+ - i_-}{2}\right) = k_s x + k_i i \tag{2.5}$$

$$u = \frac{u_+ - u_-}{2} \quad = \frac{x_0}{2i_0}\frac{\mathrm{d}}{\mathrm{d}t}\left[2L_0\frac{i_0^2}{x_0^2}x + 2L_0\frac{i_0}{x_0}\left(\frac{i_+ - i_-}{2}\right)\right] = \frac{x_0}{2i_0}\frac{\mathrm{d}}{\mathrm{d}t}F \tag{2.6}$$

$$F = 2NA\frac{i_0}{x_0}\left(\frac{B_+ - B_-}{2}\right) = 2NA\frac{i_0}{x_0}B \tag{2.7}$$

$$u = NA\frac{\mathrm{d}}{\mathrm{d}t}\left(\frac{B_+ - B_-}{2}\right) = NA\frac{\mathrm{d}}{\mathrm{d}t}B \tag{2.8}$$

Substituting force and voltage in equation (2.5) and (2.6) by the corresponding quantities in equation (2.7) and (2.8), displacement x from the nominal position can be described as a function of B, i and u.

$$x = \frac{2}{N\mu_0}\cdot\frac{x_0^2}{i_0}\cdot B - \frac{x_0}{i_0}\cdot i \tag{2.9}$$

$$x = \frac{1}{L_0}\cdot\frac{x_0}{i_0}\cdot\int u\mathrm{d}t - \frac{x_0}{i_0}\cdot i \tag{2.10}$$

Applying equation (2.9), the displacement signal x can therefore be directly calculated from the flux density B, measured for instance by a hall-effect sensor, and the current in coil i (chapter 5.1, [Zlatnik & Traxler 90]). Similarly, one could derive the displacement through current i and the integration of voltage u. From

control theory, however, it is known that the output of an integrator is not observable by its input. Thus it is not possible to reconstruct the air gap of a magnetic bearing by directly using equation (2.10). Nevertheless, it will be shown later (chapter 3.5) that, by closing the loop with the mechanical model, it becomes possible to stabilize the AMB-system by the measurements of u and i only.

Operating point		**Basic bearing constants:**	
x_0	: Nominal airgap	N	: Number of windings
i_0	: Nominal current	A	: Iron cross-sectional area
$B_0 = \frac{N\mu_0 i_0}{2 x_0}$	: Nominal flux density	($\mu_0 = 1.257 \cdot 10^{-6}$ Vs/Am	: permeability of air)
Variables (functions of time)		**Secondary bearing constants:**	
$\tilde{F}_+ ; \tilde{F}_-$	: Electromagnetic force	$L_0 = \frac{N^2 A \mu_0}{2x_0}$	: Inductance at x = const.= 0
$\tilde{B}_+ ; \tilde{B}_-$	: Flux density		
$\tilde{u}_+ ; \tilde{u}_-$	: Voltage	$k_i = 2L_0 \frac{i_0}{x_0}$	: Force-current factor
$\tilde{i}_+ = i_0 + i_+$	: Currents in the coils		
$\tilde{i}_- = i_0 + i_-$	(corresponding relations for F, B and u)	$k_s = k_i \frac{i_0}{x_0}$	: Force-displacement factor

Table 1: Notations

3. AMB-Actuator Control Configuration

An AMB-actuator usually consists of a pair of coils (fig. 1) and two power amplifiers. The actuator control configuration determines how the AMB-actuator is controlled. Starting with a general state space model of an AMB-system, the basic ideas of current, flux-density, voltage and self-sensing control are derived and discussed in this section.

State-Space Model

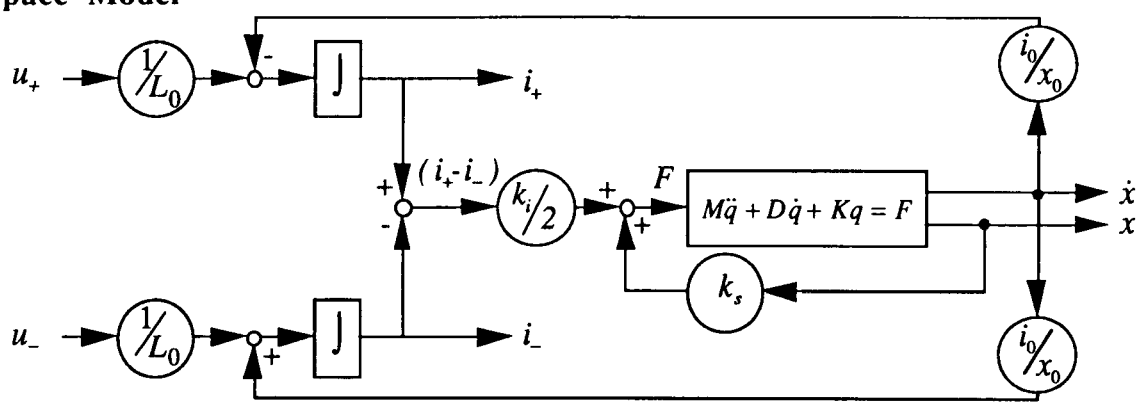

***Figure 2:** Linearized state-space model for one mechanical degree of freedom and two coils according to figure 1. The two currents (i_+, i_-),in each coil of the bearing, rotor velocity $\dot{x}$ and displacement x are selected as state variables.*

The complete state-space model for the AMB system includes at least two mechanical states (velocity and displacement). In addition, each electromagnet contributes one state variable to the model. In the case of two-sided actuators (fig. 1), two state variables, for example the currents in the coils, are necessary for each mechanical degree of freedom to completely describe the behavior of the open loop system.

Figure 2 and 3 show the state-space model of an AMB actuator acting on a general mechanical system. For simplicity we assume in chapter 3, that the mechanical system is an unbound mass m with one degree of freedom x. According to Newton's law we get the following differential equation:

$$m\ddot{x} = F \tag{3.1}$$

(For a rigid body rotor, m would stand for an equivalent rotor mass effective at the actuator.)

The MIMO-system (***Multiple Input Multiple Output***) shown in figure 2 is observable from the current measurements i_+, i_- alone. Using the voltage inputs u_+, u_-, it is also controllable. This means that the ***measurement of the rotor displacement x is not needed*** for control.

This has been demonstrated in practical setups by Vischer and in several student projects at ETH [Jordil & Volery 90], [Colloti & Kucera 91]. A patent [Vischer, Traxler & Bleuler 88] has been applied for.

A simpler state space model is found choosing B_+ and B_- as state variables rather then i_+ and i_- (fig. 3).

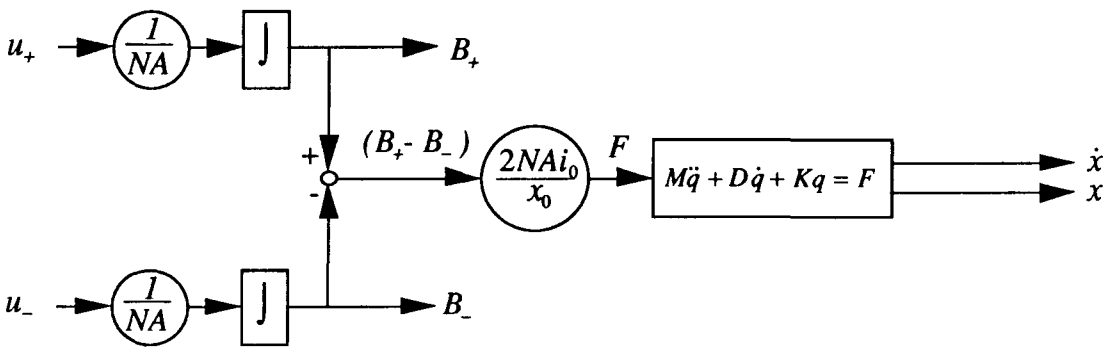

Figure 3: *Linearized state-space model for one mechanical degree of freedom and two coils according to figure 1. The two flux densities (B_+, B_-,) in each coil of the bearing, rotor velocity $\dot{x}$ and displacement x are selected as state variables.*

3.1 Voltage Control

The state space models shown in figure 2 and 3 can now be used to design a bearing control with voltage instead of current as input variable. This will be called "voltage control". Voltage control has been investigated thoroughly by many authors [Ulbrich & Anton 84], often in the context of magnetically levitated vehicles (e.g. [Jayawant 81], [Breinl 80]).

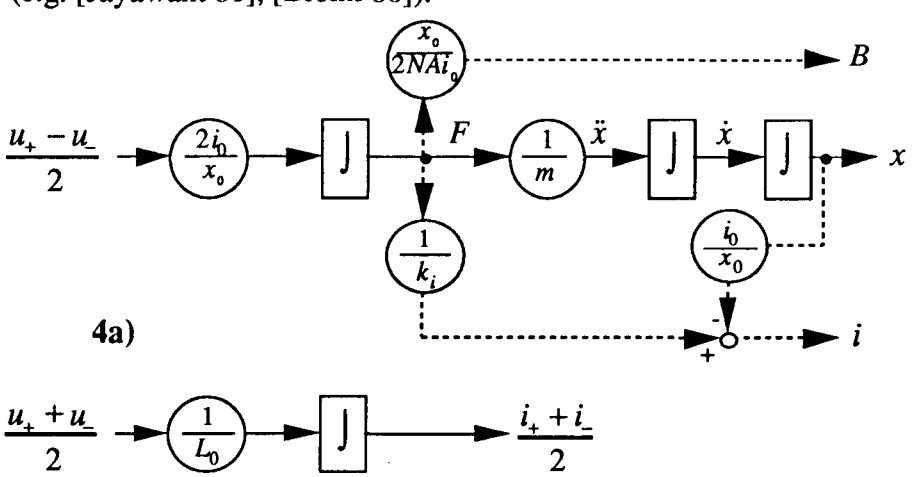

Figure 4: *Transformed state-space model for the system of figure 2 with a single mass model of the mechanical system. This choice of state variables produces two decoupled subsystems, figure 4a (with states x, $\dot{x}$ and F) and figure 4b with the single state variable $(i_+ + i_-)/2$. Figure 4b shows that the body movement only depends on the difference between the two input voltages u_+ and u_-, whereas the sum of the currents $i_+ + i_-$ is only a function of the sum $u_+ + u_-$.*

The system of figure 2 is observable if at least two of the three outputs (i_+, i_- and x) are available to the controller. The following two cases, both of which have some advantages for AMB applications, will be examined further:

- voltage control combined with three measurements (i_+, i_-, and x)
- voltage control combined with the current measurements only ("self sensing" bearing)

The system of figure 3 is observable if x and either B_+ or B_- are available to the controller.

One way to control the above systems is to implement a Luenberger observer and a state feedback controller. The full state-feedback matrix has 8 coefficients (2 inputs, 4 states). Some additional control parameters are used for the Luenberger observer. Such controllers were built and tested at ETH.

As we deal only with a single mechanical degree of freedom, we seek to simplify this controller. It is possible to describe the plant (fig. 2 and 3) as a set of two SISO-systems (Single Input Single Output), as shown in fig. 4. If the four values $(i_+ + i_-)/2$, x, $\dot{x}$ and F [Gottzein & Crämer 77] or [Gottzein et al. 77]) are used as state variables instead of i_+, i_-, x and $\dot{x}$, the MIMO-system can be replaced by a 3rd order and a first order SISO-system. The transfer function of the first subsystem (fig. 4a) is

$$x = \frac{2i_0}{x_0 m}\frac{1}{s^3}u \tag{3.2}$$

which is a simple triple integrator. The transfer function of the second subsystem (fig. 4b) is

$$\frac{i_+ + i_-}{2} = \frac{1}{L_0}\frac{1}{s}\left(\frac{u_+ + u_-}{2}\right) \tag{3.3}$$

which is a first order system independent of the rotor movement.

Thus, a controller for the voltage-controlled bearing consists of two independent sub-controllers according to the two subsystems of figure 4. For the subsystem in figure 4b a simple proportional controller is suitable. Since its main function is to keep the premagnetization current $(i_+ + i_-)/2$ at a nominal value i_0, we like to refer to it as "operating point controller".

The extension to a full order system with multiple mechanical degrees of freedom is straightforward. As seen before, each pair of opposing electromagnets is separated into two subsystems. The subsystem of figure 4b remains independent of the mechanical system.

The influence from one mechanical degree of freedom to another acts just like an ***additional force input*** at the corresponding summation points in figures 2 or 3. Decentralization, i.e. the implementation of local feedback based on a complete model, is feasible in most practical cases [Bleuler 84], with the obvious implications on the model order used for analysis. With such a layout approach, the on-line computing power requirements grow only proportional to the number of control channels.

In many cases, it is even possible to simplify one step further and to base control layout itself on a decentralized model, which brings us back to the simple models described in this chapter.

3.3 Current Control

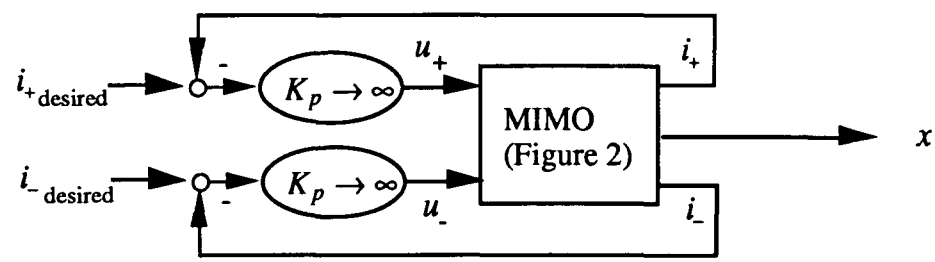

Figure 5: AMB-system with current controlled actuator

Strictly speaking, the term "current-controlled bearing" designates a special voltage-controlled bearing consisting of two current controllers as inner loops and a position control as outer loop. Because magnet current in reality is a state variable, the dynamics of the inner control loop is usually neglected for treatment of the outer loop with current as plant-input.

The inner control loops keep the two currents at their desired values, which is possible as long as the voltages are not saturated and the assumption of infinite inner loop gains K_P is legitimate. The transfer characteristic is given by equation (2.5) as

$$i_{+\text{desired}} = i_+ \text{ and } i_{-\text{desired}} = i_- \Rightarrow F = k_s x + k_i\left(\frac{i_+ - i_-}{2}\right) = k_s x + k_i i \tag{3.4}$$

Equation (3.4) shows that the current controlled bearing can be interpreted as a *"force-source"*, which is not entirely perfect due to the undesirable term ($k_S\, x$) corresponding to a spring with a negative stiffness k_S. This negative stiffness term only turns up in the context of current control.

3.4 Flux Density Control

Quite similar to the current control, the flux density measurements can also be used to directly control the flux densities B_+ *and* B_- in the air-gaps to desired values by means of two inner loops, as shown in figure 6.

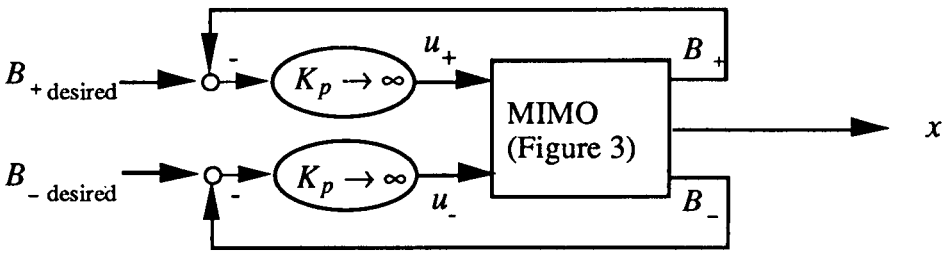

***Figure 6:** AMB-system with flux density controlled actuator*

The behavior of the flux density controlled bearing is then given by equation 2.7.

$$B_{+\text{desired}} = B_+ \text{ and } B_{-\text{desired}} = B_- \Rightarrow F = 2NA\frac{i_0}{x_0}\left(\frac{B_+ - B_-}{2}\right) = 2NA\frac{i_0}{x_0}B \tag{3.5}$$

The advantages of this actuator control configuration is that it yields an almost perfect *"force-source"* without the negative bearing stiffness associated with the current control. Furthermore the relation between force and flux density is linear, as opposed to current control and voltage control, where the assumed equations are only valid around the operating point and some other specific locations in the work space.

As we could see in equation (2.9), the displacement x can be calculated from the flux density and the current in the coil. This type of indirect displacement measurement is excellently suited for large air gaps (chapter 5.1).

3.5 Comparison of Actuator Control Configurations

Current control has the advantage that the two states associated with the two magnetic coils can be neglected under certain conditions (see chapter 3.3). It makes the design of the main controller a little easier (e.g. PD control is feasible).

When voltage control is employed, only one of the two states is taken care of by an inner actuator loop, whereas the second state has to be considered in the layout of the main controller.

Voltage controlled AMBs, however, have the advantages that the open loop system has no negative stiffness k_S (highly instable open loop system). It is known from control theory, that a highly instable open

loop system is very sensitive to time lag and noise in the measurement. Detailed description can be found in [Vischer 88]. Future comparison involving other criteria is shown in figure 7.

Criteria	Voltage Control	Current Control	Flux Control
Sensitivity to Timelag in the Measurement	⇧	⇩	⇧
Sensitivity to Noise in the Measurement	⇧	⇩	⇧
Copper Resistance	▬	⇧	⇧
Stray Field	▬	⇧	⇧
Saturation of Iron	⇧	⇩	⇧
Validity of Linearization	▬	▬	⇧

⇧ Advantage ▬ Minor Disadvantage ⇩ Disadvantage

Figure 7: Comparison of actuator control configurations

Flux density control: *Force-source* (eq. 2.2)

Current Control: "*Force-source*" & negative stiffness (eq. 2.5)

Voltage control: "*Force derivative source* " if the the rotor is approximated by one mass (eq 2.7 and 2.8)

3.5 Self-Sensing AMB

The transfer function (3.8) from input $u=(u_+-u_-)/2$ to output $i=(i_+-i_-)/2$ nicely shows the operating principle and the feasibility of the self-sensing bearing.

$$i = \frac{\frac{1}{L_0}s^2 - \frac{2i_0^2}{x_0^2 m}}{s^3} u \tag{3.8}$$

Both transfer functions (3.3) & (3.8) are of full order; therefore it can be deduced that the voltage controlled AMB-plant is observable and controllable from the measurements of the current (i_+-i_-) and i only.

Figure 8 shows the corresponding simple state-space model.

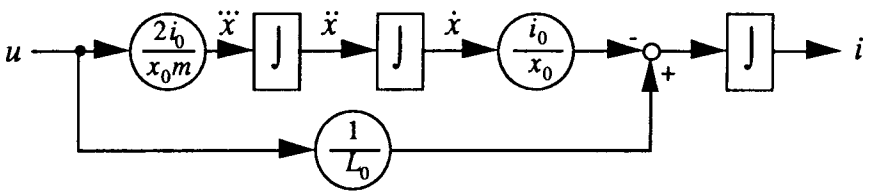

Figure 8: Transformed state-space model of the SISO-plant of figure 4 for self-sensing operation. (State variables: $i=(i_1-i_2)/2$, $\dot{x}$ and $\ddot{x}$) This system together with the subsystem of figure 4b can be used to design a simple linear controller for the self-sensing bearing.

It can be shown, that the simplest linear main controller for the self-sensing bearing is

$$u = \frac{b_2 s^2 + b_1 s + b_0}{a_1 s + a_0} i \tag{3.9}$$

4. DESIGN OF THE MAIN CONTROLLER

The controller is generally a part of a mechatronic (electro-mechanical) system. It feeds back some sensed signals of the system to the actuators of the system. Thus, the controller is involved with the whole system and can never be regarded isolated. The system design starts with the design of the plant and the design and placement of the sensors and actuators, called control configuration. Next, an appropriate model of the system has to be derived and control layout specifications have to be defined. Thereby, the modelling and the control design cannot be treated as separate problems [Skelton 89]. After the controller layout, the controller has to be implemented and tested.

Thus, the main controller layout is only a part of the whole AMB-system design and has to be done in tight cooperation with rotor design, sensor and actuator design and placement, modelling and implementation. The good controller layout leads only to good performance if the system configuration (actuator, sensor, mechanical structure etc.) is optimized.

AMB-systems can usually be modelled as quite linear systems, even if the AMB-actuator is not absolutely linear. A suspended flexible structure can lead to a high order model. We therefore assume, that the plant, P, and the controller, C, are linear and time-invariant (LTI).

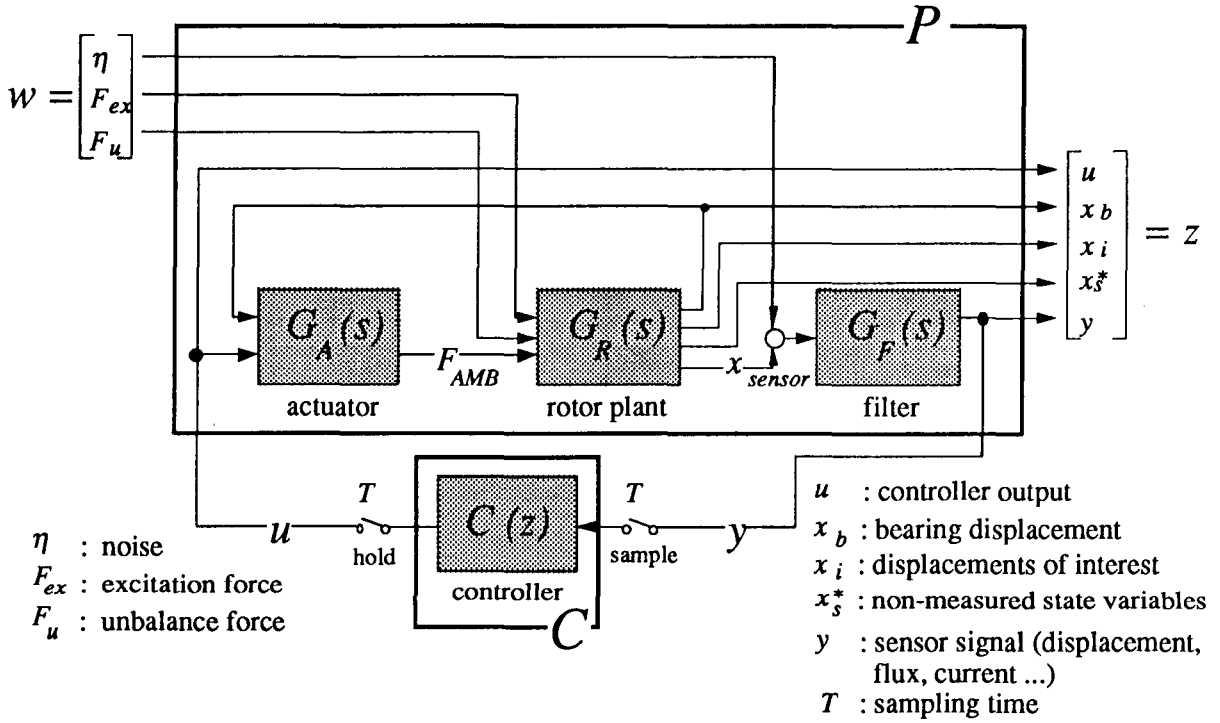

***Figure 9:** Block scheme of a typical AMB-system*

Figure 9 shows a general AMB system, where $G_A(s)$ is the transfer matrix of the AMB-actuator, $G_R(s)$ that of the rotor plant (suspended body) and $G_F(s)$ that of the sensor and signal filtering. The transfer matrices $G_A(s)$, $G_R(s)$ and $G_F(s)$ describe the AMB-plant P. C(z) is the transfer matrix of the controller C which has to be designed. The controller C is assumed to be time discrete.

The inputs to the plant are divided into two vector signals:

- The *actuator input vector* ***u***, consisting of those inputs to the plant which can be manipulated by the controller.
- The *exogenous input vector* ***w***, consisting of all other input quantities such as noise, excitation forces, etc.

The output of the plant consists of two vector signals:

- The *measured output vector* **y**, consisting of those measured signals which are accessible to the controller.
- The *regulated output vector* **z**, consisting of all outputs of interest such as actuator input, rotor displacements, measured and non measured state variables.

This notation of the plant includes more details about the AMB system than is common in classical control [Boyd et al. 90]. The exogenous inputs and regulated variables contain each signal subject to constraints or specification, whether it is measured or not.

Some general examples of specifications for AMB-systems can be found in the next paragraph.

4.1 Specifications for the Controller Layout

The controller layout of an AMB system is always restricted by different specifications. The specifications have to be defined by the AMB-engineer and include e.g. physical aspects of the plant and specifications on the system performance. Common examples are:

closed loop stability

maximum stiffness over a given frequency band [Herzog & Bleuler 90]

limitation of the amplifier's bandwith [Keith et al. 90], [Siegwart & Traxler 90]

noise rejection, noise filtering

force free rotation around the inertial axis [Higuchi et al 90]

damping to cross critical speed

vibration rejection

robustness (changes in the plant, modelling errors, nonlinearities)

The constraints and specifications often define upper and lower bounds for the input-output behavior of the AMB-system shown in figure 9.

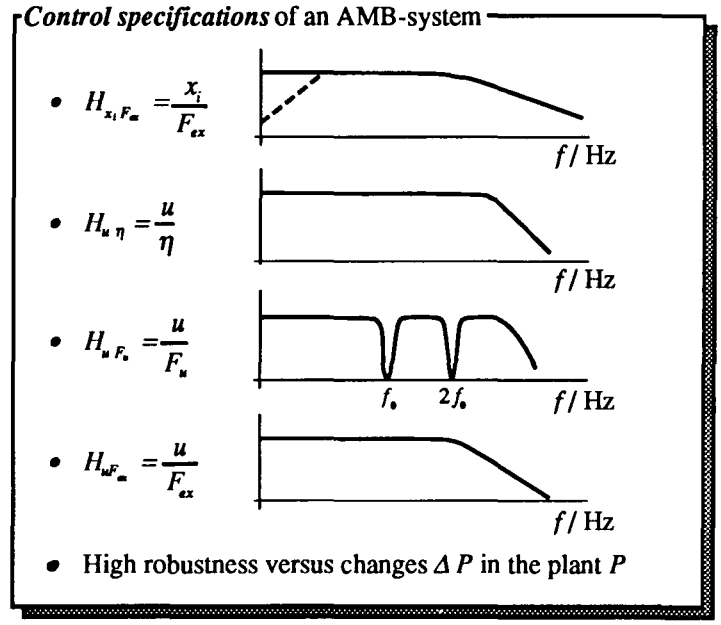

***Figure 10:** An example for the specifications given for an AMB system.*

Possible specifications of input-output transfer function of AMB-systems are shown in figure 10. Unfortunately, the different specifications often are in opposition to each other. It is up to the talented control engineer to find an acceptable compromise. After defining the bounds of the controller layout, different *design tools* help to find an optimal solution to the control problem.

4.2 On Different Controller Design Approaches

Modern AMB controllers will almost certainly make use of digital control with its well-known advantages such as large flexibility in controller structure changes during machine installation or easy implementation of additional controller features ("feedforward" control, automatic adaptation to changing plant parameters, machine monitoring etc.).

In the process of controller design, the control engineer has either to find a control law that meet the design specifications (chapter 4.1) or determine that none exists. If there is no controller meeting the specifications, the control engineer has to change the specifications and/or the system configuration. Thus, a good controller design tool should allow an account of all design specifications of the given design problem and consider the specific control configuration of the system.

Specific control features of AMB systems are:

- only very few system states, most often the displacements at the coils, are measured.
  $\Rightarrow$ observer based controller (LQG, LQR, H^2, H^∞)
- the controller often has to be of much lower order than an adequate plant model
  $\Rightarrow$ direct low order controller design (PD, PID, SPOC-D)
- many control specifications have to be considered (see chapter 4.1)
  $\Rightarrow$ H^∞, 'convex optimization' of the class of all stabilizing controller, SPOC-D

Many different control approaches for linear and time-invariant (LTI) are available and it is up to the control engineer to choose the most appropriate to solve his control problem. Some of them, namely the PD, PID, LQG, LQR and the more advanced direct low order controller design (SPOC-D) and H^∞ methods are discussed in the following.

PD, PID controller layout

PD and PID controllers are the most common and most used controllers. The basic idea is to use a feedback similarly to 'a mechanical spring and damper'. The big advantages are, that they are easy to understand and easy to implement (even in analog technique). In many applications they are fairly robust due to the positive real transfer function of a PD controller. However, with PD and PID the controller has always to be decentralized for MIMO-systems. Only very few specifications can be met by PD / PID controllers and closed-loop stability can not be guaranteed. PD / PID is a predefined low order approach which does usually not account for high demanding specifications of high order plants.

Observer Based High Order Controller

As stated before, a typical property of many practical AMB systems is the fact that only very few system states, most often the displacements at the AMB-coils, are measured. This is the case especially with flexible rotors, where the order of an appropriate plant model is much higher than the number of sensor signals available. The well-known consequence is:

A *high order* observer-based state feedback must be implemented including the full dynamics of the plant. Stability and good performance of the nominal closed-loop system may then be achieved by an appropriate controller design method such as the well-known LQR and LQG methods (Linear Quadratic Riccati resp. Linear Quadratic Gaussian).

One crucial drawback of this controller design approach, however, is that this high order control scheme will require a considerable amount of computation time for the estimation of the non-measured state variables and for the calculation of the corresponding controller output signals. The consequence is either the need of a sophisticated and expensive multi-processor or the acceptance of low sampling rates whenever single-processor implementations are used.

Hence, *low order* discrete-time *dynamic output control schemes* must be sought in order to simplify the control task. The most general approaches for such a *low order controller* are summarized in figure 12:

Controller Reduction and Practical Aspects of Low Order Controller Implementation:

According to figure 11 the three basic ways to achieve a practically implementable discrete-time controller are:

- model reduction prior to the controller design
- controller reduction after controller design
- direct low order controller design

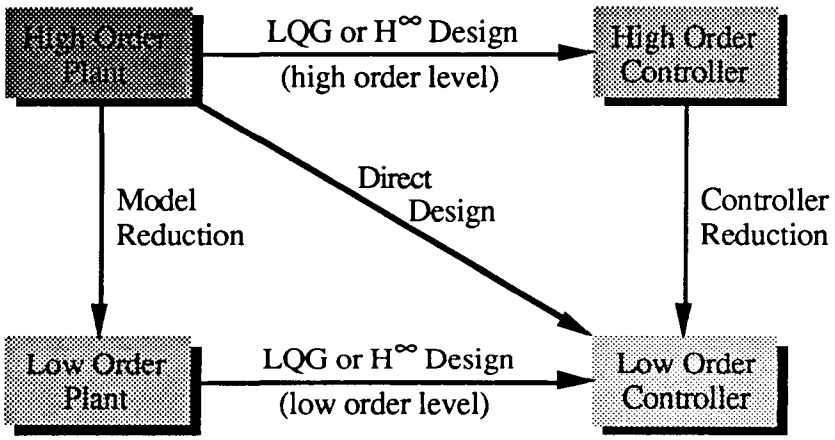

***Figure 11:** Basic principles of low order controller design (figure from [Anderson & Liu 89])*

Many among the first two mentioned reduction techniques can be denoted as so called "open-loop" reduction methods. This means that stability of the resulting closed-loop system is *not* an intrinsic property of the reduction process. A practical example, well-known to any AMB control engineer, is that *high frequency bending eigenmodes* will often turn out to be unstable when reduced order controllers or controllers relying on reduced models are used.

> The common way out of this is post layout on-site "tuning" of the nominal AMB controller or filtering of non-desired signal components by means of notch-filters in the feedback loop

Both listed approaches of a practical implementation of reduced AMB controllers are quite *ineffective*: On the one hand, "tuning" is a time-intensive and therefore expensive job, and obtained results can hardly be transferred to any other type of machine. On the other hand, notch-filtering of bending eigenmodes has a drastically deteriorating impact on the overall controller performance, since the necessary controller phase lead is degraded even in the rigid body (i.e. low frequency) range. Thus, the use of notch-filters makes the following controller tuning a necessary task, and, roughly spoken, renders the preceding LQR or LQG controller layout often very unqualified.

> Another, more sophisticated way is to account for the neglected plant dynamic in the controller design specifications. Such specifications can be included in H^∞ and 'convex optimization' of the class of all stabilizing controller.

This approach seems very promising, especially because all neglected plant dynamic of the real physical plant, not only of an appropriate model, can be included in the control specifications.

Direct Design of Low Order Dynamic Compensators:

A promising and most practical solution to the problem of obtaining *low order controllers* for *high order plants* is the *direct low order controller design*: [Bernstein & Hyland 84], [Larsonneur 90]:

Order and *structure* of the discrete-time controller for the nominal high order (i.e. not reduced) plant model are *predefined prior to the controller layout* (structurally constrained controller). This predefinition is made according to practical needs such as physical considerations, complexity constraints, decentralization, symmetry etc.

This approach is, in fact, very common in AMB applications where, quite often, discrete-time low order approximations of traditional continuous-time P(I)D control schemes are implemented. The most simple discrete-time PD approximations are the following ones (controller output u, measured plant output y, sampling time T, time event k, proportional respective differential control coefficients P and D):

$$u_i(k) = \left(P + \frac{D}{T}\right) y_i(k) - \frac{D}{T} y_i(k-1) \tag{4.1}$$

$$u_i(k) = \left(P + \frac{3D}{2T}\right) y_i(k) - \frac{4D}{2T} y_i(k-1) + \frac{D}{2T} y_i(k-2) \tag{4.2}$$

Such P(I)D controller schemes exactly match above direct design definition: the controller order (e.g. 1st or 2nd order) and a decentralized structure (sensor signal y_i is fed back on actuator input u_i only) are predefined prior to the controller layout (determination of P resp. D). The control parameters P and D can then be obtained by numerical simulations or, again, by on-site "tuning" of the AMB system.

In many cases, no set of control parameters (P,D) can be found stabilizing both low frequency rigid body and higher frequency bending eigenmodes. More sophisticated approaches for direct low order controller design, namely the so called SPOC-D approach, are therefore required (see next paragraph).

4.3 Structure-Predefined Optimal Control for Discrete Systems (SPOC-D)

Lately, a direct low order controller design method for discrete-time systems named SPOC-D (*Structure-Predefined Optimal Control for Discrete Systems*) has been developed at the Swiss Federal Institute of Technology (ETH). This method has a strongly practical orientation. Similar to the LQR/LQG design methods, SPOC-D uses a quadratic performance criterion to be optimized, accounting for a high order plant model as well as for the controller dynamics. The fundamental difference to these classical methods, however, is that the controller order and structure are *not a result* of the controller design process, as it is the case for LQR/LQG or familiar methods, where high order plants generally lead to high order controllers (see figure 11). The SPOC-D method combines the advantages of a system optimization including the full plant dynamics on the one hand and possibly simple low order dynamic compensator schemes on the other hand and, thus, closes the gap between the classical LQR/LQG or pole placement methods and the more practical and less sophisticated P(I)D approaches.

The main features of SPOC-D can be summarized as follows:

- discrete-time controller order and structure are freely predefinable according to practical needs (low or high order, fully coupled or completely decentralized, etc.)
- determination of an optimal set of control parameters by minimizing a quadratic performance criterion involving both, the full plant and the controller dynamics
- analytical description of the performance criterion (by Lyapunov equations) and corresponding vector gradient allowing for an efficient numerical optimization process
- consideration of *additional* linear or nonlinear *control specifications* in order to achieve specific controller properties of practical importance (stiffness, noise reduction at high frequencies, band pass filtering, symmetries, etc.)

A detailed description of the SPOC-D method is not presented in this paper but can be found in [Larsonneur 90]. However, controller layout results for a high speed AMB milling spindle are presented in chapter 5.3.

4.4 H^∞: A MiniMax Approach to Control

Cultural Remarks and Motivation for H^∞ Control

An intuitively most appealing motivation for H^∞ control is supplied by its differential game analogy [Doyle et al. 89]: consider a plant with two inputs. These two inputs which are also called players are set up in opposition. The first player *u(t)* (that's you in fact !) is the control input generated by the controller (your strategy). The second player *w(t)* (your adversary) is an *exogenous* input signal which could represent some disturbance. Of course, this exogenous input signal is a priori unknown to you; the only available signal for the controller input is the measured plant output *y(t)*. Your objective is to *minimize* the *"worst case"* disturbance, that is to *minimize* the disturbance which causes the *maximal* "damage" (in terms of energy) to the plant output *z(t)*. This *"minimax"* optimization problem characterizes H^∞ control. Note that figure 9 in section 4 exactly matches the situation described above.

Practical Aspects of Designing and Implementing H^∞ Controllers

The *off-line* effort for computing H^∞ controllers has been drastically reduced recently by the "state space approach" in [Doyle et al. 89], where the resulting controller is basically given in terms of two algebraic Riccati equations. H^∞ software packages are already available [Matlab], and algorithms are being improved and standardized. These advances have a common desirable consequence: the H^∞ approach is nowadays available to a broader section of the control community. However, there is still a computational *on-line* burden because standard H^∞ designed MIMO (multiple input multiple output) controllers are fully coupled, and their order is roughly the same as the order of the plant. That is why there remains a strong need to keep up with the latest developments in special purpose controller architectures, in modern "closed-loop" controller reduction schemes [Anderson & Liu 89], [Mustafa & Glover 91], and in decentralized control [Wu 90].

Experimental implementations of H^∞ designed controllers for AMB systems (especially for high performance AMB milling spindles) will be effectuated soon at our institute. The AMB milling spindle is a particularly challenging application example of H^∞ control since the cutting forces of the milling process appear as a highly unpredictable exogenous input which may cause intolerable vibrations of the milling tool. Some theoretical considerations to this problem were carried out in [Herzog & Bleuler 90]. In [Matsumura et al. 90] experimental results based on the H^∞ "mixed sensitivity" approach were shown. A theoretical example is shown in chapter 5.4.

5. Theoretical and Experimental Results

5.1 Displacement Sensing by Flux Density Measurement

The laboratory prototype crystal-growth system shown on figure 13 makes use of equation (2.9) for the displacement measurement [Zlatnik & Traxler 90]. The flux density measurement together with a current measurement is used for the displacement sensing. The lack of a special displacement sensor is specially useful for large air-gaps, lower costs and encapsulated rotor systems. A liquid phase epitaxy centrifuge in a similar arrangement and with a totally encapsulated rotor, is currently installed at MECOS Traxler AG. The temperature at the front end of the rotor goes up to 800° Celsius.

5.2 Self-sensing AMB Systems

One way to build a self-sensing bearing is to design a Luenberger observer for the voltage controlled system of 4th order according to figure 4. The observer can be tuned by comparing the estimated air gap with the measurement of a position sensor. A state feedback can then be implemented and self-sensing operation is achieved by switching position feedback from the measured signal to the estimated one. This was implemented in [Jordil & Volery 90] on a signal processor with a sampling time of 120 µs.

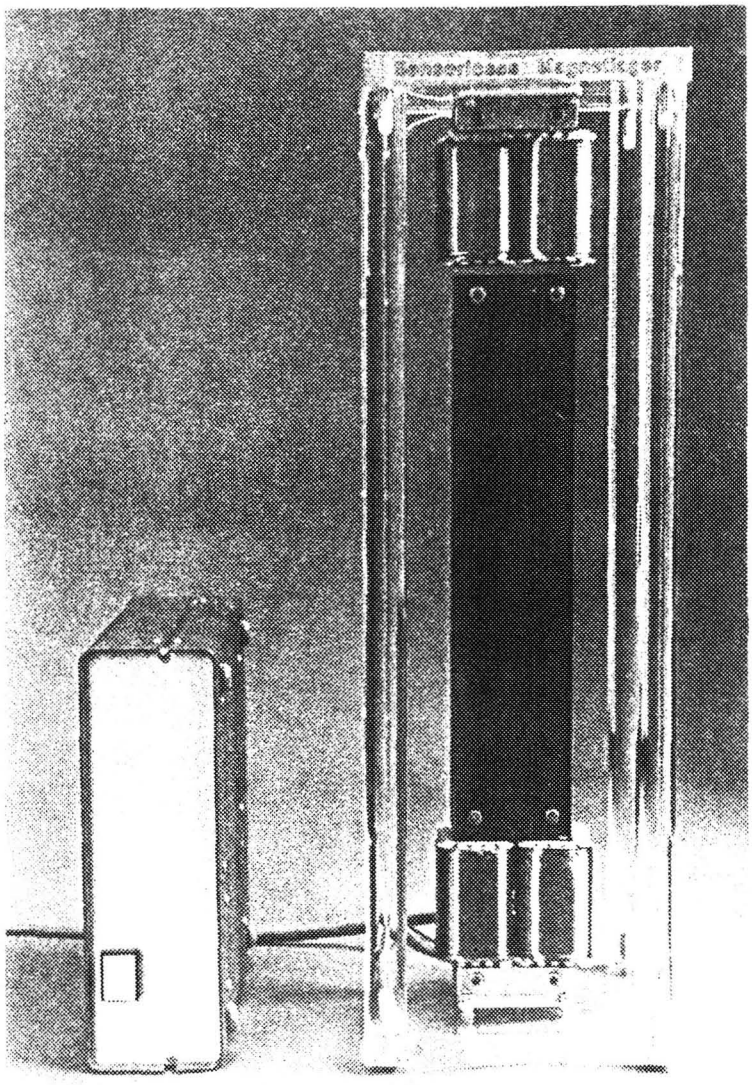

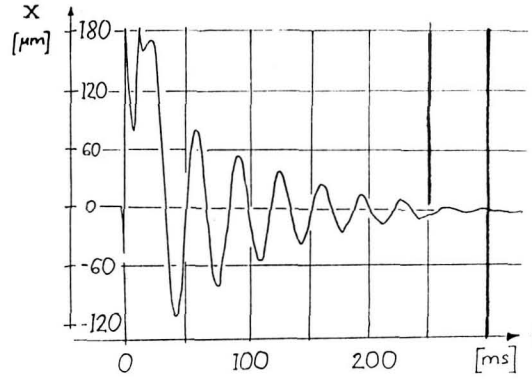

Figure 12a: *Demonstration model of the self sensing bearing with one controlled degree of freedom. The Box on the right contains power amplifier, power supply and controller.*

Figure 12b: *Measurement of impact response (hammer) of position signal of a self-sensing AMB. The air gap of the bearing is 0.7 mm, rotor mass is 8 kg, bearing diameter is 78 mm, bias current is 0.5 A and maximum force is over 100N. The static behavior is satisfactory, similar to the current controlled bearing. The dynamic response is still not exciting, and has to be improved.*

An analog realization of a self-sensing bearing was successfully completed as a student project [Colloti & Kucera 91]. The controller makes use of the separation shown in figure 4. The complete circuit needs very few electronic components. A good robustness of the bearing was achieved.

The measurement result of figure 12 shows the system response to an impact force, a blow with a hammer on the rotor. Maximum rotor displacement of this measurement was about 0.3 mm which is almost maximum rotor clearance in the auxiliary bearing and about 50% of the total air gap in the bearing magnet. Further technical data of this system is given in the figure caption

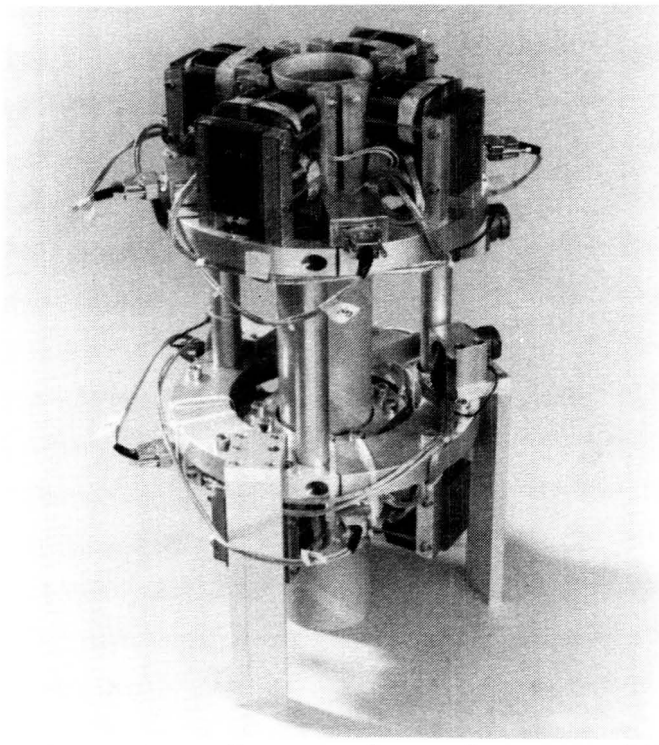

Figure 13 *Laboratory set-up of a crystal-growth system with displacement sensing by flux and current measurement.*

5.3 Optimal Control of a Stiff AMB System using the SPOC-D Method

The example in this chapter is from an actually realized system, a high performance AMB milling spindle, controlled by a single digital signal processor (DSP) [Siegwart et al. 90]. It illustrates the large variety of control goals offered by the SPOC-D method.

The procedure to obtain an appropriate controller fulfilling the desired requirements can be summarized as follows (see details in [Larsonneur 90]):

1. Step: Predefinition of discrete-time controller structure and order according to the practical feasibility. For the milling spindle example, two decentralized dynamic compensators, each of 4th order, have been chosen (sampling frequency 10kHz). This yields the following IIR (*Infinite Impulse Response*) controller transfer function in the z-domain:

$$g(z) = \frac{u(z)}{y(z)} = \frac{d_0 + d_1 z^{-1} + d_2 z^{-2} + d_3 z^{-3} + d_4 z^{-4}}{1 + c_1 z^{-1} + c_2 z^{-2} + c_3 z^{-3} + c_4 z^{-4}} \qquad G(z) = \begin{bmatrix} g_1(z) & 0 \\ 0 & g_2(z) \end{bmatrix} \tag{4.3}$$

   Note that this controller predefinition uses two decentralized 4th order controllers $g(z)$ for a plant of *total order 14* (including sensor and anti-aliasing filter state variables), and involves *only 18 control coefficients*, whereas a full state observer for this plant would require *56 control coefficients* and corresponding multiplications.

2. Step: Introduction of *additional control specifications* in order to achieve requirements of *important practical relevance*. Here, the *static bearing stiffness* (without integrator feedback), *suppression of rotation-synchronous AMB force components* (analogous to notch-filters) and *noise suppression* at high frequencies are introduced as parameter constraints. This results in an *interdependence* of the control parameters. For the given case, four control coefficients of each dynamic compensator will be dependent on the other five.

   Note that the conditions of bearing stiffness, unbalance and noise suppression or other parameter constraints are *directly* introduced into the controller design process *before*

optimization and not achieved by any specific choice of weighting matrices during the controller optimization process.

3. Step: Determination of the independent and dependent control parameters by numerical minimizing a quadratic performance criterion (which includes the parameter constraint equations). Efficient numerical minimizing procedures can be used since vector gradients are formulated analytically.

The resulting controller transfer function of this optimization process for the AMB milling spindle is shown in the following figure:

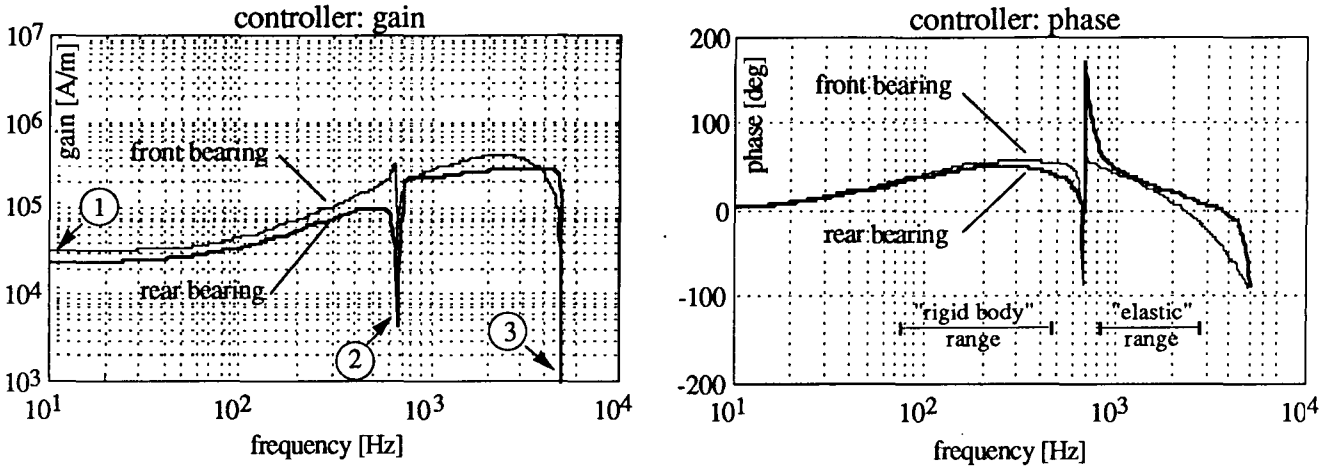

Figure 14: *Transfer functions of the SPOC-D optimized decentralized discrete-time controller (4th order) at rear and front AMB of the high speed milling spindle. The conditions of static bearing stiffness (1), unbalance force suppression (2) and noise suppression (3) are introduced by control parameter constraints.*

As can be seen from above results the SPOC-D optimized decentralized low order controller perfectly accounts for the the desired spindle requirements: high stiffness, unbalance and noise suppression and large "damping" (positive controller phase lead) in the low frequency rigid body range as well as in the higher frequency bending eigenmode range. This is made possible by optimally using the design freedom offered by low order dynamic compensators in a most practical and straightforward way, instead of "tuning" otherwise obtained controllers so that they match the desired requirements.

5.4 Stiff AMB Control: H^∞ versus PD

Comparing different controller layout methods is not an easy task. Clearly, any comparison must be made with respect to a *common* performance index. There is an erroneous and prejudiced opinion stating that PD controllers are mostly "nearly optimal" in "some" sense, and that modern control theory only allows small "performance improvements" at the expense of extremely high sophistication. Our illustrative example here proves the contrary.

Consider the controlled AMB system in figure 15. The two mass oscillator P stands for a simple electromagnetically supported *flexible* shaft. The system is assumed to be subjected to an *unknown* disturbance force $w(t)$ acting on the bottom mass m_1. Let $z(t)$ denote the displacement of m_1 caused by $w(t)$, and let $T(s)$ be the frequency-domain compliance: $z(s) = T(s)\, w(s)$. Let the objective of controller $C(s)$ be to stabilize $P(s)$ and to maintain the magnitude of dynamic compliance $|T(i\omega)|$ uniformly below a given bound α, i.e. $|T(i\omega)| < \alpha$ for all frequencies ω. The main feature of this example is that the disturbance and actuator forces are *not* acting on the *same* mass. This implies the following drawback for PD control $C(s) = -(p + d\,s)$: *neither* low *nor* high (p, d) gains are appropriate for very stiff control, i.e. for a small value of α. Note that high (p, d) gains lead to a *rigid top* mass m_2, whereas the *bottom* mass m_1 is nearly *undamped*, which produces a high resonance peak of dynamic compliance $|T(i\omega)|$.

Obviously, "optimal" (p, d) tuning leads to investigating $\max_\omega |T(i\omega)|$ as a function of (p, d), see figure 16. It can be concluded from this example that PD controllers may give poor performance results especially

if the actuator and disturbance forces are not acting on the same place. Now, what is the answer of H^∞ to all this? In [Herzog & Bleuler 90] we derived the following result:

> For the above example, there exist stabilizing controllers $C(s)$ enabling an *arbitrarily* low compliance peak bound $\alpha > 0$.

Of course, a low value of α implies high controller authority. Actually there is a *trade-off* between *several* requirements. This trade-off reasoning is absolutely fundamental to control engineering. PD control disguises this fact since high *(p, d)* gains do not necessarily lead to high performance. The freedom offered by PD tuning is only a tiny little subset of the freedom offered by the set of all stabilizing controllers. However, if the performance specifications are *not* very demanding, the reduced freedom of PD controllers is mostly sufficient.

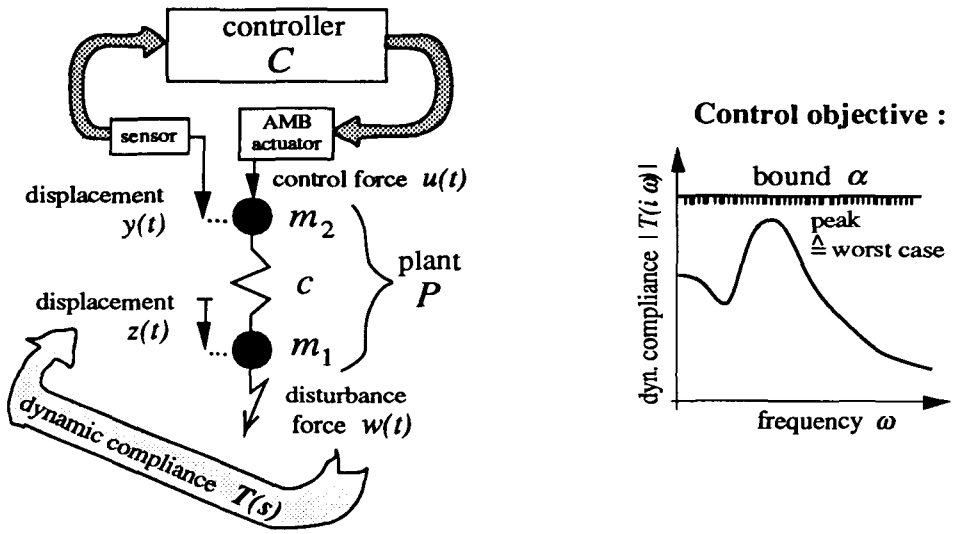

Figure 15: *Control problem and objective*

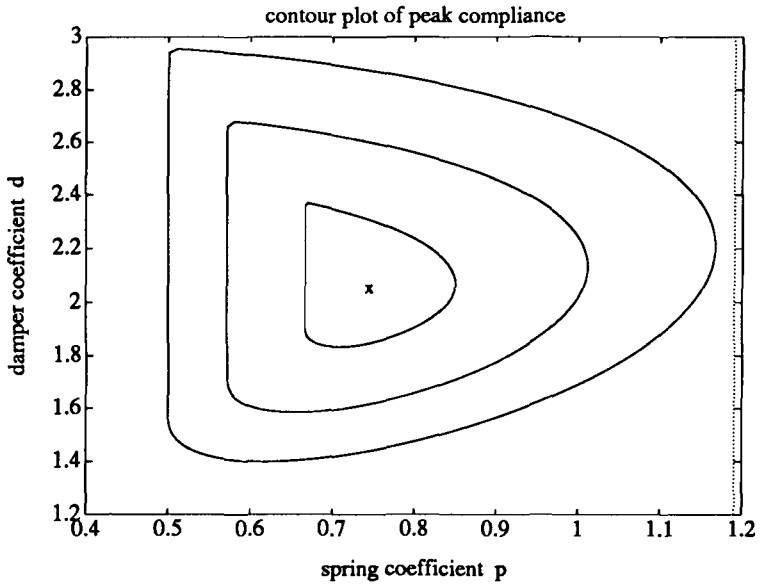

Figure 16: *Contour plot for the following peak level values: {3, 2.75, 2.5}. The cross marks the optimum (p, d) tuning* $p_{opt} \approx 0.7444$, $d_{opt} \approx 2.0478$. *The corresponding (p, d)-optimal peak compliance is about* $\max_\omega |T(i\omega)| \approx 2.3438$. *Parameter values of plant P:* $m_1 = m_2 = c = 1$.

6. Conclusion and Outlook

Various control configurations of AMB-actuators have been presented. Voltage and flux density control are promising for many applications, advantages are clearly indicated by theory. Extended experimental comparisons remain to be done.

A self-sensing AMB has been presented in theory and realization, i.e. an AMB using no sensing hardware in the bearing [Bleuler & Vischer 91]. Self-sensing AMB are a promising solution for low cost applications or applications where conventional sensing hardware is expensive.

The control layout is regarded as a key point of AMB system design. However, a good control layout alone cannot guarantee a good system behavior when the "*conditioning*" of the control plant is bad.

New approaches to control design as they have been outlined in this paper have many advantages compared to the widely used PD and PID control. With new control design tools such as *direct low order controller design* [Larsonneur 90] , H^∞ or *'convex optimization' over the set of all stabilizing controllers* [Boyd et al. 90], controller specifications can be met, which are not achievable by PD/PID or even by LQG/LQR approaches. Some examples show the advantages of the new design techniques.

A successful control layout, especially for high performance systems, is still a very challenging engineering problem. There are thousands of problems to be solved. New AMB-systems, with better control configurations have to be designed, better sensor and actuator hardware has to be developed and new control design methods have to be investigated. To improve the performance of AMB systems it is essential that the whole system is treated as a mechatronic product where all parts are interdependent. Not the isolated design of AMB components, but smart integration of all parts into the overall system will result in successful products.

7. References

[Anderson & Liu 89] Anderson B.D.O and Liu Y.: Controller Reduction: Concepts and Approaches, IEEE Transactions on Automatic Control, Vol. 34, No. 8, pp. 802-812, 1989

[Beams et al. 46] Beams J.W., Young J.L. and J.W. Moore: The Production of High Centrifugal fields, Journ. of Appl. Physics, Vol 17, pp 886-890, 1946

[Bernstein & Hyland 84] Bernstein D.S. and D.C. Hyland: The Optimal Projection Equations for Fixed-Order Dynamic Compensation, IEEE Trans. AC, Vol. 29, No. 11, 1984

[Bleuler 84] Bleuler H: Decentralized Control of Magnetic Bearing Systems, Doctor thesis no 7573, ETH Zürich 84

[Bleuler & Vischer 91] Bleuler H., Vischer D.: Magnetic Bearing Systems with Minimal Hardware Requirement, ROMAG '91 Magnetic Bearing & Dry Gas Seals, Int. Conf., Alexandria Va., March 91

[Boyd et al. 90] Boyd S., Barratt C. and S. Norman: Linear Controller Design: Limits of Performance Via Convex Optimization, Proceedings of the IEEE, Vol. 78, March 1990.

[Breinl 80] Breinl W.: Entwurf eines unempfindlichen Tragregelsystems für ein Magnetschwebefahrzeug. Fortschrittbericht der VDI-Zeitschriften, Reihe 8, Nr. 34, München, 1980.

[Colloti & Kucera 91] Colloti A. and L. Kucera: Low Cost Magnetic Bearings, Semesterarbeit IfR 1991.

[Doyle et al. 89] Doyle J.C., Glover K., Khargonekar P.P., and B. A. Francis: State Space Solutions to Standard H^2 and H^∞ Control Problems, IEEE Trans. AC, Aug. 1989, Vol. 34, No. 8, p. 831-847.

[Gottzein & Crämer 77] Gottzein E. and W. Crämer: Critical Evaluation of Multivariable Control Techniques based on MAGLEV Vehicle Design. IFAC Symposium on Multivariable Technological Systems, Canada, July 1977.

[Gottzein et al. 77] Gottzein E., Miller L. and R. Meisinger: Magnetic Suspension Control System for High Speed Ground Transportation Vehicles. World Electrical Congress, Moscow, June 1977.

[Herzog & Bleuler 90] Herzog R. and H. Bleuler: Stiff AMB Control using an H^∞ Approach, 2nd Int. Symp. on Magnetic Bearings, Tokyo 1990

[Higuchi et al. 90] Higuchi T., Mizuno T. and M. Tsukamoto: Digital Control System for Magnetic Bearings with Automatic Balancing, 2nd Int. Symp. on Magnetic Bearings, Tokyo 1990

[Jayawant 81] Jayawant B.V.: Electromagnetic Levitation and Suspension Techniques, London, Arnold, 1981

[Jordil & Volery 90] Jordil P. and F. Volery: Régulation d'un palier magnétique sans senseur de position, Student's diploma project, Feb. 1990, Inst. for Robotics, ETH Zürich

[Keith et al. 90] Keith F.J., Maslen E.H., Humphris R.R., and R.D. Williams: Switching Amplifier Design for Magnetic Beaarings, 2nd Int. Symp. on Magnetic Bearings, Tokyo 1990

[Larsonneur 90] Larsonneur R.: Design and Control of Active Magnetic Bearing Systems for High Speed Rotation, Doctoral Thesis No. 9140, ETH Zürich, 1990

[Matlab] Chiang R.Y. and M.G. Safonov: User's Guide of the Robust Control MATLAB Toolbox, The Mathworks Inc., Natick, MA 01760

[Matsumura et al. 90] Matsumura F., Fujita M. and M. Shimizu: H^∞ Robust Control Design for a Magnetic Suspension System, 2nd Int. Symp. on Magnetic Bearings, Tokyo 1990

[Mustafa & Glover 91] Mustafa D. and K. Glover: Controller Reduction by H^∞ Balanced Truncation, IEEE Trans. AC, June 1991, Vol. 36, No. 6, p. 668-682.

[Siegwart & Traxler 90] Siegwart R. and A. Traxler: Performance and Limits of AMB-Actuators Illustrated on an Electromagnetically Suspended Milling Spindle, Proc. 25th Intersociety Energy Conversion Engineering Conference. Nevada, August 1990

[Siegwart et al. 90] Siegwart R., Larsonneur R. and A. Traxler: Design and Performance of a High Speed Milling Spindle in Digitally Controlled Active Magnetic Bearings, 2nd Int. Symp. on Magnetic Bearings, Tokyo 1990

[Skelton 89] Skelton R.E.: Model Error Concepts in Control Design, Int. J. Control, Vol. 49, No. 5, 1989

[Traxler 85] Vischer D.: Eigenschaften und Auslegung von berührungsfreien elektromagnetischen Lagern, Doctor Thesis No. 7851, ETH Zürich, 1985

[Ulbrich & Anton 84] Ulbrich H. and E. Anton: Theory and Application of Magnetic Bearings with Integrated Displacement and Velocity Sensors, The Inst. of Mech. Eng., C299/84, Cambridge 1984

[Vischer 88] Vischer D.: Sensorlose und spannungsgesteuerte Magnetlager, Doctor Thesis No. 8665, ETH Zürich, 1988

[Vischer, Traxler & Bleuler 88] Vischer D., Traxler A., Bleuler H.: "Magnetlager", patent No. 678090, 22.11.88, Switzerland

[Wu 90] Wu Q.: An Application of H^∞ Theory to Decentralized Robust Control, thesis ETH Zurich, No. 9116

[Zlatnik & Traxler 90] Zlatnik D. and A. Traxler: Cost-Effective Implementation of AMB, 2nd Int. Symp. on Magnetic bearings, Tokyo, 1990